Oncogene (2015), 1–11

www.nature.com/onc

ORIGINAL ARTICLE

LKB1 deficiency enhances sensitivity to energetic stress induced by erlotinib treatment in non-small-cell lung cancer (NSCLC) cells

YM Whang[1], SI Park[2], IA Trenary[1], RA Egnatchik[1], JP Fessel[3], JM Kaufman[4], DP Carbone[5] and JD Young[1,6]

The tumor suppressor serine/threonine kinase 11 (*STK11* or *LKB1*) is mutated in 20–30% of patients with non-small-cell lung cancer (NSCLC). Loss of LKB1-adenosine monophosphate-activated protein kinase (AMPK) signaling confers sensitivity to metabolic inhibition or stress-induced mitochondrial insults. We tested the hypothesis that loss of LKB1 sensitizes NSCLC cells to energetic stress induced by treatment with erlotinib. LKB1-deficient cells exhibited enhanced sensitivity to erlotinib *in vitro* and *in vivo* that was associated with alterations in energy metabolism and mitochondrial dysfunction. Loss of LKB1 expression altered the cellular response to erlotinib treatment, resulting in impaired ATP homeostasis and an increase in reactive oxygen species. Furthermore, erlotinib selectively blocked mammalian target of rapamycin signaling, inhibited cell growth and activated apoptosis in LKB1-deficient cells. Erlotinib treatment also induced AMPK activation despite loss of LKB1 expression, which was partially reduced by the application of a calcium/calmodulin-dependent protein kinase kinase 2 inhibitor (STO-609) or calcium chelator (BAPTA-AM). These findings may have significant implications for the design of novel NSCLC treatments that target dysregulated metabolic and signaling pathways in LKB1-deficient tumors.

Oncogene advance online publication, 29 June 2015; doi:10.1038/onc.2015.140

INTRODUCTION

Lung cancer is the leading cause of cancer-related mortality worldwide and is linked to 28% of all cancer-related deaths in the United States.[1] Despite advances in traditional therapeutic strategies involving surgery, ionizing radiation therapy, and chemotherapy, the 5-year survival remains less than 20%.[2] In recent years, it has become clear that non-small-cell lung cancer (NSCLC) has a high frequency of somatically acquired genetic alterations that define critical subsets of tumors with distinct behaviors.[3] An improved understanding of potential vulnerabilities of lung cancer subsets has led to the development of effective targeted therapies for tumors with certain activated oncogenes,[4,5] but little is known about specific susceptibilities that may derive from the loss of classical tumor suppressor genes, such as *LKB1*.

LKB1 is a tumor suppressive serine/threonine kinase that activates diverse downstream kinases, thus regulating a variety of cellular phenotypes including metabolism, invasion, proliferation and polarity.[6] *LKB*1 inactivation occurs in 20–30% of lung adenocarcinomas,[7] and *LKB1* deficiency in combination with *KRAS* mutation leads to an aggressive tumor phenotype at high prevalence in mouse models, surpassing that of *KRAS* mutation alone.[8] Many of the metabolic regulatory functions of LKB1 are mediated by its interaction with adenosine monophosphate-activated protein kinase (AMPK). LKB1 phosphorylates and activates AMPK,[6] which functions to regulate cellular energy metabolism under conditions of low ATP.[9] AMPK also contributes to inactivation of mammalian target of rapamycin (mTOR) when ATP levels fall, which leads to inhibition of protein synthesis and cell growth.[10] Therefore, loss of LKB1 leads to dysregulation of cellular metabolism and cell growth under conditions of energy stress,[11] resulting in enhanced sensitivity to drug treatments that target bioenergetic pathways.[12]

Most lung cancers express the epidermal growth factor receptor (EGFR), and this signaling pathway is the major target of several drugs in the clinic. EGFR tyrosine kinase inhibitors including gefitinib and erlotinib have been shown to suppress oncogenic signaling through downstream pathways such as PI3K-Akt-mTOR and MAPK/extracellular signal-regulated kinase (Mek)-extracellular signal-regulated kinase (Erk).[13] NSCLC tumors with certain activating mutations in *EGFR* show enhanced sensitivity to these compounds.[14] However, the majority of NSCLC patient tumors possess wild-type *EGFR*, with only 10–30% harboring a mutant *EGFR* allele.[15] Although erlotinib has clear therapeutic efficacy in some NSCLC tumors bearing wild-type *EGFR*[16,17] and is approved for patients with wild-type *EGFR* tumors,[18] it is unclear how to best identify which of these patients may benefit from treatment with EGFR-targeted inhibitors. Furthermore, the mechanism by which erlotinib induces selective cell death in wild-type *EGFR* tumors is not completely known.

In *EGFR* mutant NSCLC cells, erlotinib causes apoptosis through activation of intrinsic pathways mediated by the induction of BH3-only BIM protein or activation of caspase 3.[19,20] In these studies, erlotinib treatment was associated with loss of mitochondrial

[1]Department of Chemical and Biomolecular Engineering, Vanderbilt University, Nashville, TN, USA; [2]Center for Bone Biology, Division of Clinical Pharmacology, Department of Medicine, Vanderbilt University, Nashville, TN, USA; [3]Division of Allergy, Pulmonary, and Critical Care Medicine, Department of Medicine, Vanderbilt University, Nashville, TN, USA; [4]Department of Cancer Biology, Vanderbilt University, Nashville, TN, USA; [5]Department of Internal Medicine, The Ohio State University Medical Center, Columbus, OH, USA and [6]Department of Molecular Physiology and Biophysics, Vanderbilt University, Nashville, TN, USA. Correspondence: Professor JD Young, Department of Chemical and Biomolecular Engineering, Vanderbilt University, PMB 351604, Nashville, TN 37235, USA.
E-mail: j.d.young@vanderbilt.edu
Received 15 September 2014; revised 19 February 2015; accepted 20 March 2015

potential, which resulted in mitochondrial-mediated apoptosis. Interestingly, recent studies suggest that LKB1 deficiency causes an accumulation of defective mitochondria and loss of mitochondrial membrane potential, resulting in depletion of hematopoietic stem cells through disruption of mitophagy and mitochondrial homeostasis.[21] Furthermore, the mitochondrial complex I inhibitor phenformin enhanced apoptosis of LKB1-deficient tumor cells by depletion of mitochondrial membrane potential compared with wild-type LKB1-reconstituted cells.[12] Therefore, we hypothesized that erlotinib would be more effective at inducing apoptosis in LKB1-deficient NSCLC cells because of disruption of normal mitochondrial function, even in the presence of wild-type *EGFR*.

In the present study, we tested whether LKB1-deficient cells were more prone to apoptosis in response to erlotinib treatment, both *in vitro* and *in vivo*, in the absence of mutationally activated EGFR. Our data demonstrate enhanced antitumor effects of erlotinib in LKB1-deficient cells that are associated with loss of mitochondrial function and blockage of mTOR signaling. Overall, our findings suggest that the LKB1-deficient molecular phenotype may serve as a predictive marker for erlotinib sensitivity and, if substantiated by further studies, may provide a rationale for the therapeutic use of erlotinib to treat LKB1-deficient NSCLC. This is significant because LKB1 mutations are preferentially found in NSCLC tumors with wild-type EGFR,[22,23] and thus LKB1 loss may define a novel subset of tumors with enhanced erlotinib sensitivity that is largely distinct from the classical subset possessing targetable EGFR mutations.

RESULTS

LKB1-deficient cells are more sensitive to inhibition of EGFR-PI3K-mTOR signaling

We sought to determine the relative inhibitory effects of erlotinib, as well as other compounds that target the EGFR-PI3K-mTOR signaling pathway, across a panel of NSCLC cell lines that express either wild-type or mutant LKB1. The expressions of LKB1and EGFR were assessed by western blotting in NSCLC cells (Figure 1a). The NSCLC cells tested have been reported to express wild-type EGFR,[24,25] and the expression level of phosphorylated EGFR is shown in Figure 1a. Calu-6, H2009 and H358 cells were previously reported to express wild-type LKB1,[26–28] and we confirmed LKB1 protein expression in these three lines. Next, we asked whether erlotinib could selectively inhibit the viability of LKB1 mutant cells harboring *KRAS* mutations but with wild-type *EGFR*. We found that LKB1 mutant cells were more sensitive to erlotinib on average (Figure 1b). Furthermore, 10 μM of the PI3K inhibitor LY294002 did not reduce viability of LKB1wild-type NSCLC cells, whereas 30–50% inhibition was observed in LKB1 mutant cells. Sensitivity to rapamycin was also exacerbated in LKB1 mutant cells. We further assessed the survival of NSCLC cells using a colony-forming assay where cells were pretreated with inhibitor for 72 h and then grown in inhibitor-free medium for 2 weeks. The colony-forming assay was more capable of detecting differences in viability at low inhibitor concentrations and confirmed the finding that LKB1 mutant cells were more sensitive to inhibition of EGFR-PI3K-mTOR signaling (Figure 1c). These results suggest that LKB1 loss confers enhanced sensitivity to inhibition of the EGFR-PI3K-mTOR signaling pathway in NSCLC cells harboring wild-type *EGFR*.

LKB1-deficient transgenic cells exhibit increased sensitivity to erlotinib treatment

A549 and H460 cells (both wild-type *EGFR* and mutant *LKB1*) were transduced with retroviral constructs to stably express wild-type LKB1 or an empty vector control. Expression of LKB1 and related downstream signaling proteins was verified in these stable transgenic cells (Figure 2a, left). LKB1 phosphorylates Thr172 in the activation loop of AMPKα[29,30] and activates AMPK under

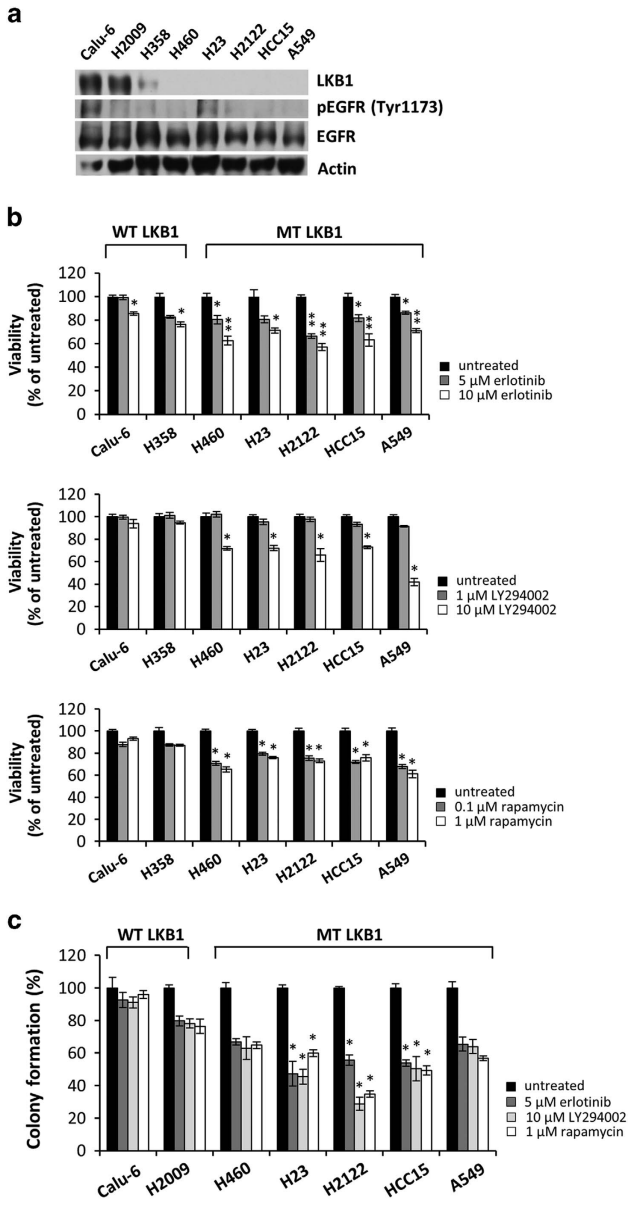

Figure 1. Erlotinib and inhibitors of PI3K-mTOR signaling selectively inhibit growth of LKB1-deficient NSCLC cells. (**a**) Levels of LKB1 expression and EGFR phosphorylation in our panel of NSCLC cells. Actin was used as a loading control. (**b**) Effect of treatment with erlotinib, LY294002 or rapamycin on viability of NSCLC cells. Cells were seeded in 96-well plates. After 24 h, cells were treated with indicated concentrations of erlotinib, LY294002 or rapamycin for 48 h. Cell viability was determined using MTT assay. $^{*}P < 0.005$, $^{**}P < 0.00001$, untreated/erlotinib, $^{*}P < 0.0001$, untreated/LY294002 or untreated/rapamycin. Data are mean ± s.e.m. ($n = 6$). (**c**) Effects of treatment with erlotinib, LY294002 or rapamycin on colony-forming ability of NSCLC cells. After 72 h treatment with erlotinib, LY294002 or rapamycin, cells were re-plated in 12-well plates at low density. Colonies were counted after 2 weeks of growth. $^{*}P < 0.0001$, untreated/erlotinib, untreated/LY294002, or untreated/rapamycin. Data are mean ± s.e.m. ($n = 3$).

elevated AMP levels.[31] Activated AMPK subsequently phosphorylates and inhibits acetyl-CoA carboxylase (ACC). Overexpression of LKB1in A549 and H460 resulted in increased basal phosphorylation of AMPKα and its downstream target ACC. Erlotinib inhibited the growth of LKB1-nonexpressing A549 ($P < 0.0001$) and H460 cells ($P < 0.005$) more than it did the growth of LKB1-

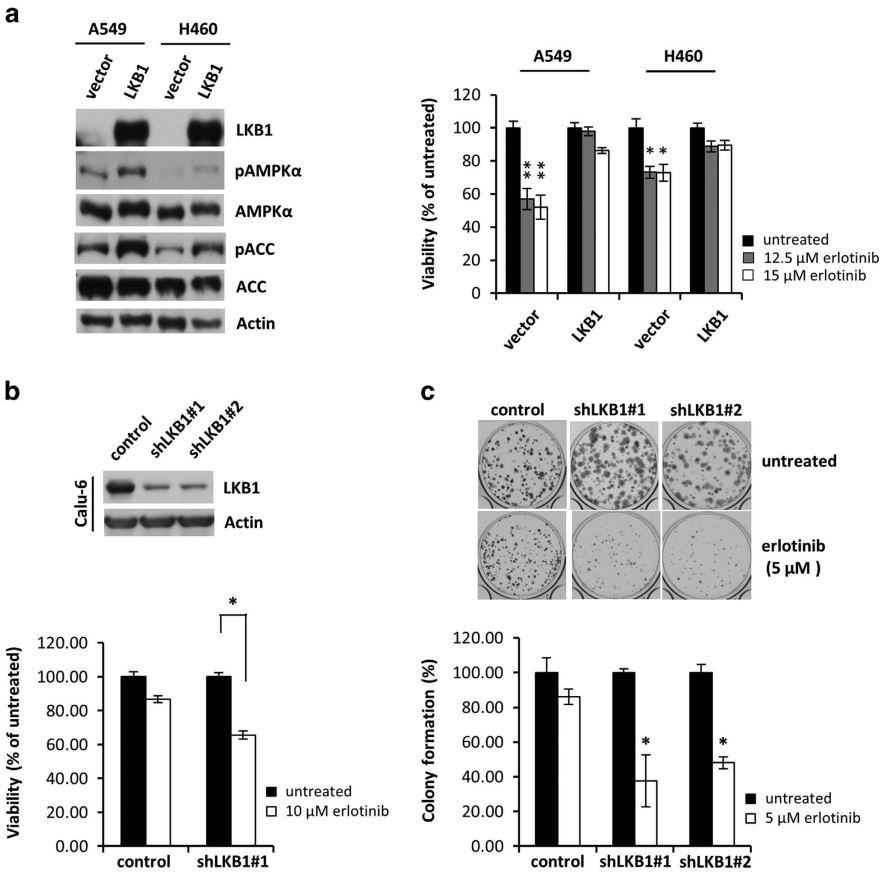

Figure 2. Erlotinib selectively inhibits growth of LKB1 mutant cells and LKB1 knockdown cells. (**a**) Left panel: levels of LKB1 expression and LKB1-related downstream proteins in A549 and H460 cells stably expressing empty pBABE vector (vector) or wild-type LKB1 (LKB1). Right panel: cell viability determined by MTT assay. Cells were treated with indicated concentrations of erlotinib for 48 h. $^{*}P < 0.005$, $^{**}P < 0.0001$, untreated/erlotinib. Data are mean ± s.e.m. ($n = 6$). (**b**) Upper panel: western blots of whole-cell lysates from LKB1 stable knockdown and non-targeted shRNA control Calu-6 cells after puromycin selection: control, pLKO.1 control vector; shLKB1#1 and shLKB1#2, LKB1 shRNA vectors. Lower panel: cell viability determined by MTT assay. $^{*}P < 0.0001$, untreated/erlotinib. Data are mean ± s.e.m. ($n = 6$). (**c**) Colony-forming ability of LKB1 stable knockdown Calu-6 cells. After 72 h treatment with 5 μM erlotinib, cells were replated in 12-well plates at low density. Colonies were counted after 2 weeks of growth. $^{*}P < 0.001$, untreated/erlotinib. Data are mean ± s.e.m. ($n = 3$).

overexpressing cells (Figure 2a, right). Conversely, in stable LKB1-knockdown lines generated from LKB1 wild-type Calu-6 cells, erlotinib induced a more substantial reduction in growth compared with the vector control (Figure 2b, lower panel). In addition, erlotinib reduced the colony-forming ability of LKB1-knockdown cells more significantly than the vector control (Figure 2c). These results suggest that LKB1 deficiency enhances sensitivity to erlotinib by suppressing the viability and tumorigenic potential of NSCLC cells.

Erlotinib treatment selectively inhibits oxidative metabolism and disrupts energy homeostasis in LKB1-deficient cells

We next determined whether erlotinib treatment alters cellular metabolism through analysis of glucose, lactate and oxygen exchange rates. Knockdown of LKB1 in Calu-6 cells caused basal glucose consumption and lactate production to increase significantly compared with vector control cells (Figure 3a, left), consistent with previously published results.[32] Measurement of oxygen consumption rate (OCR) also revealed a twofold increase in basal oxidative metabolism by shLKB1 Calu-6 cells (Figure 3b, upper), which was further confirmed in shLKB1 H358 cells (Supplementary Figure S1A). Erlotinib treatment reduced specific growth rates of both vector control and shLKB1 Calu-6 cells in a dose-dependent manner without affecting glucose uptake or lactate production (Figure 3a, left). However, the OCR of shLKB1-expressing Calu-6 and H358 cells was halved by erlotinib treatment (Figure 3b and Supplementary Figure S1A). Similar results were observed after re-expressing LKB1 in A549 and H460 cells. LKB1 mutant A549 and H460 cells exhibited increased glucose consumption and lactate production compared with LKB1-overexpressing cells (Figure 3a, right and Supplementary Figure S2). Furthermore, OCR was significantly elevated in LKB1 mutant cells but was reduced >50% by erlotinib treatment (Figure 3b and Supplementary Figure S1B). In contrast to its effects on glycolytic metabolism, the effect of erlotinib to reduce OCR was significantly enhanced in the LKB1 mutant lines.

The reduction in OCR by erlotinib treatment was associated with a significant increase in the ADP/ATP ratio in shLKB1-expressing Calu-6 and H358 cells (Figure 3c). In contrast, the OCR and ADP/ATP ratio of control Calu-6 and H358 cells was not significantly affected by erlotinib. These results indicate that LKB1-deficient cells were not able to maintain their elevated rate of oxidative phosphorylation in the presence of erlotinib treatment, thus leading to ATP depletion. Several recent articles have shown that loss of LKB1 function leads to increased expression of mitochondria-associated genes[23] but also induces defective mitophagy and accumulation of dysfunctional mitochondria.[12,21] Therefore, we hypothesized that

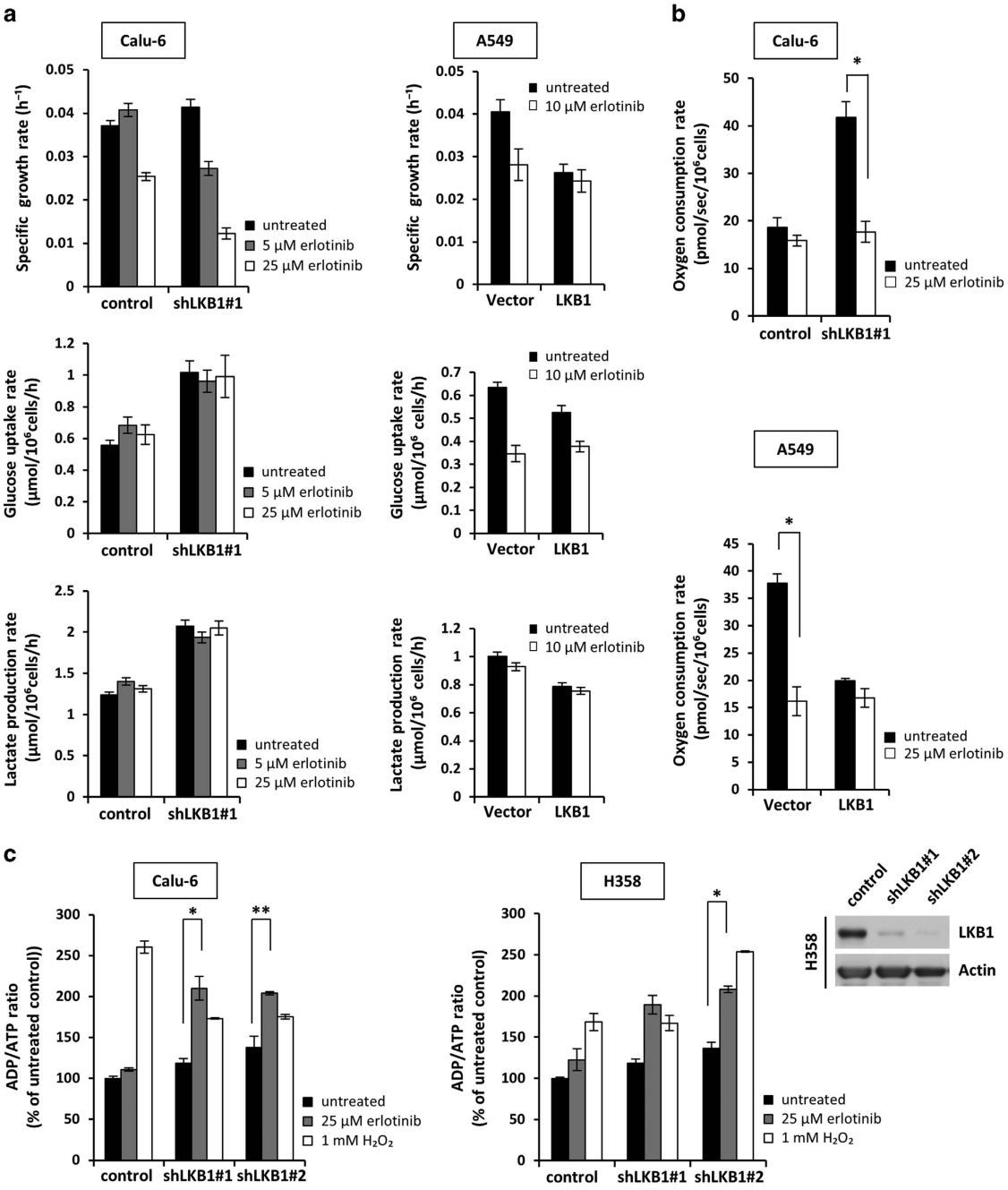

Figure 3. Erlotinib reduces growth rate and selectively inhibits oxidative phosphorylation in LKB1-deficient cells. (**a**) Cell growth rate, glucose uptake rate and lactate production rate of Calu-6 and A549 cells. Cells were grown for 72 h in the presence of treatments. (**b**) OCR of Calu-6 and A549 cells. Cells were treated with erlotinib for 24 h. Data are mean ± s.e.m. ($n = 4$). *$P < 0.005$, untreated/erlotinib. (**c**) Left panel: ADP/ATP ratio of Calu-6 and H358 cells. Cells were treated with 25 μM erlotinib for 24 h or 1 mM H_2O_2 (positive control) for 1 h before measurement. Right panel: western blot analysis of LKB1 expression in H358 cells. Data are mean ± s.e.m. *$P < 0.05$, **$P < 0.005$, untreated/erlotinib.

mitochondrial impairments may have a role in the response of LKB1-deficient cells to erlotinib treatment.

Erlotinib treatment unmasks mitochondrial defects in LKB1-deficient cells

Erlotinib-induced apoptosis is associated with loss of mitochondrial membrane potential in *EGFR* mutant NSCLC cells.[20] Therefore, we sought to determine whether *EGFR* wild-type NSCLC cells bearing loss-of-function mutations in LKB1 would show similar mitochondrial defects following erlotinib treatment. We measured the effect of erlotinib treatment on mitochondrial potential by using the cationic dye JC-1. Phenformin, a mitochondrial complex I antagonist, was applied as a positive control to impair mitochondria. As shown in Figure 4a, following treatment with erlotinib or phenformin, Calu-6 and H358 cells expressing shLKB1 exhibited enhanced dissipation of $\Delta\psi_m$ compared with control cells (red to green ratio of JC-1), reflecting impaired mitochondrial membrane integrity. Significantly, the $\Delta\psi_m$ of untreated shLKB1 cells was higher than that of vector controls, which is indicative of increased basal mitochondrial activity and is consistent with the elevated OCR of untreated shLKB1 cells (Figure 3b). Calu-6 cells

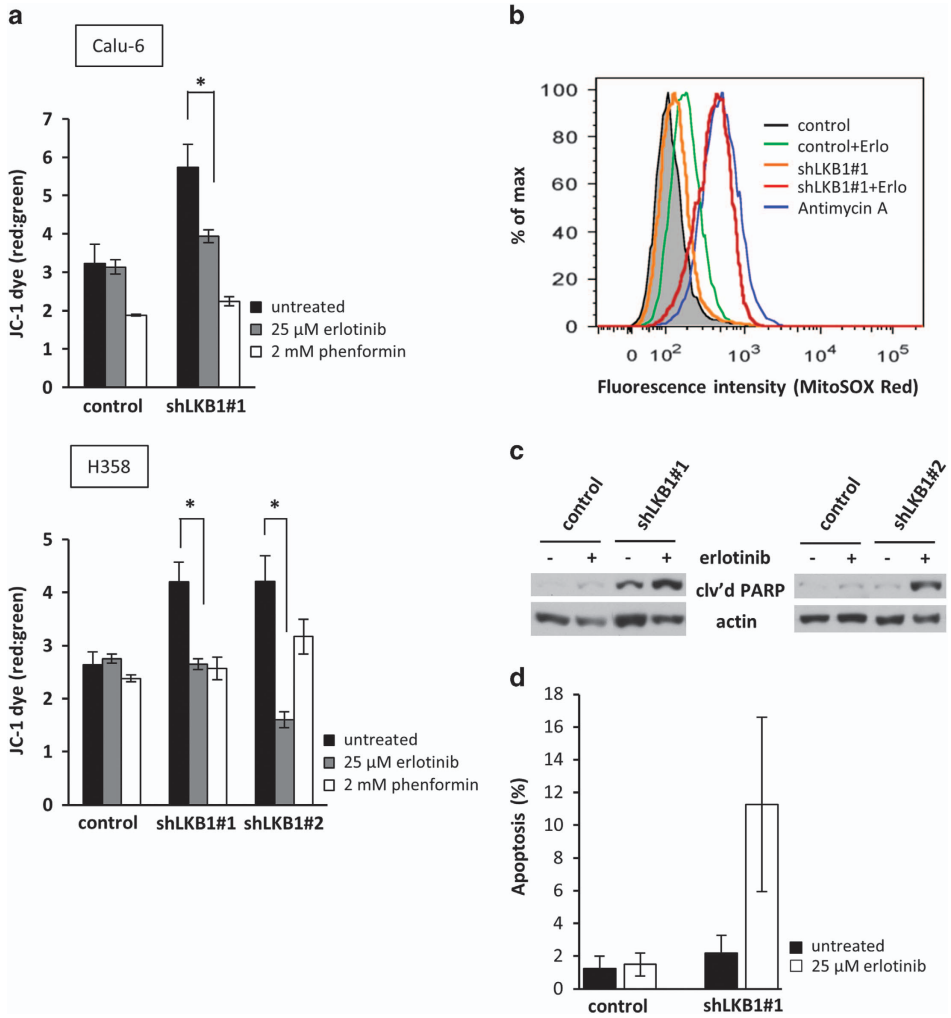

Figure 4. Erlotinib induces mitochondrial defects and enhanced apoptosis in stable LKB1 knockdown NSCLC cells. (**a**) Mitochondrial potential was measured using JC-1 fluorescence in both Calu-6 and H358 cells. Cells were treated with 25 μM erlotinib for 24 h. Data are mean ± s.e.m. *$P < 0.05$, untreated/erlotinib. (**b**) Mitochondrial ROS accumulation by Calu-6 cells. Cells were treated with 25 μM erlotinib for 24 h or with 20 μM antimycin A (positive control) for 40 min before staining with MitoSOX Red and analysis by flow cytometry. (**c**) Induction of apoptosis by erlotinib in Calu-6 cells. Control and shLKB1 cells were treated with 25 μM erlotinib for 24 h and cell lysates were subjected to western blot analysis using antibody to cleaved PARP. (**d**) Apoptosis was detected with Annexin V staining in control and shLKB1 Calu-6 cells following 48 h treatment with erlotinib.

expressing shLKB1 also exhibited increased mitochondrial production of reactive oxygen species (ROS) in response to erlotinib treatment (Figure 4b). We hypothesized that ATP depletion, loss of mitochondrial membrane potential, and ROS accumulation might be associated with increased apoptosis in LKB1-deficient cells. As shown in Figures 4c and d, treatment of shLKB1 Calu-6 cells with erlotinib induced cleavage of poly(ADP-ribose) polymerase (PARP) and an accumulation of apoptotic cells, suggesting that erlotinib enhances mitochondrial-mediated apoptosis in LKB1-deficient cells. These data indicate that LKB1-deficient cells rely more heavily on mitochondria for energy metabolism under basal conditions, but they exhibit profound mitochondrial dysfunction in response to erlotinib treatment as evidenced by $\Delta\psi_m$ collapse, ATP depletion, ROS accumulation and apoptosis activation.

Erlotinib activates AMPKα and blocks mTOR signaling in LKB1-deficient cells

Next, we evaluated the effect of erlotinib on phosphorylation of AMPKα at 3, 6 and 24 h post treatment. Interestingly, erlotinib induced phosphorylation of AMPKα after 6 h treatment in shLKB1 Calu-6 cells (Figure 5a, left panel), with increased phosphorylation of ACC apparent by 24 h. A similar increase in ACC phosphorylation was observed after 24 h treatment in shLKB1 H358 cells (Supplementary Figure S3). This effect was not observed in the control cells. In non-transgenic LKB1 mutant NSCLC cells, erlotinib also induced phosphorylated AMPKα in both H23 and H460 cells after 3 h treatment (Figure 5a, right panel). These results indicate that AMPKα remains sensitive to changes in ATP levels induced by erlotinib treatments in spite of reduced or abolished LKB1 activity. To confirm the effect of erlotinib to suppress EGFR activation and signaling through downstream pathways, we performed western blot analysis of EGFR, Akt and mTOR phosphorylation in the presence of exogenous EGF (Figure 5b). EGF treatment stimulated phosphorylation of EGFR and Akt in both control and shLKB1 cells. EGFR phosphorylation was effectively reduced by erlotinib treatment in both cell types, but only shLKB1 Calu-6 cells exhibited reduced phosphorylation of mTOR in response to erlotinib. Therefore, we hypothesized that activation of AMPKα in LKB1-deficient cells might confer sensitivity to erlotinib through inhibition of mTOR signaling. As shown in Figure 5c, erlotinib induced phosphorylation of AMPKα in both control and shLKB1

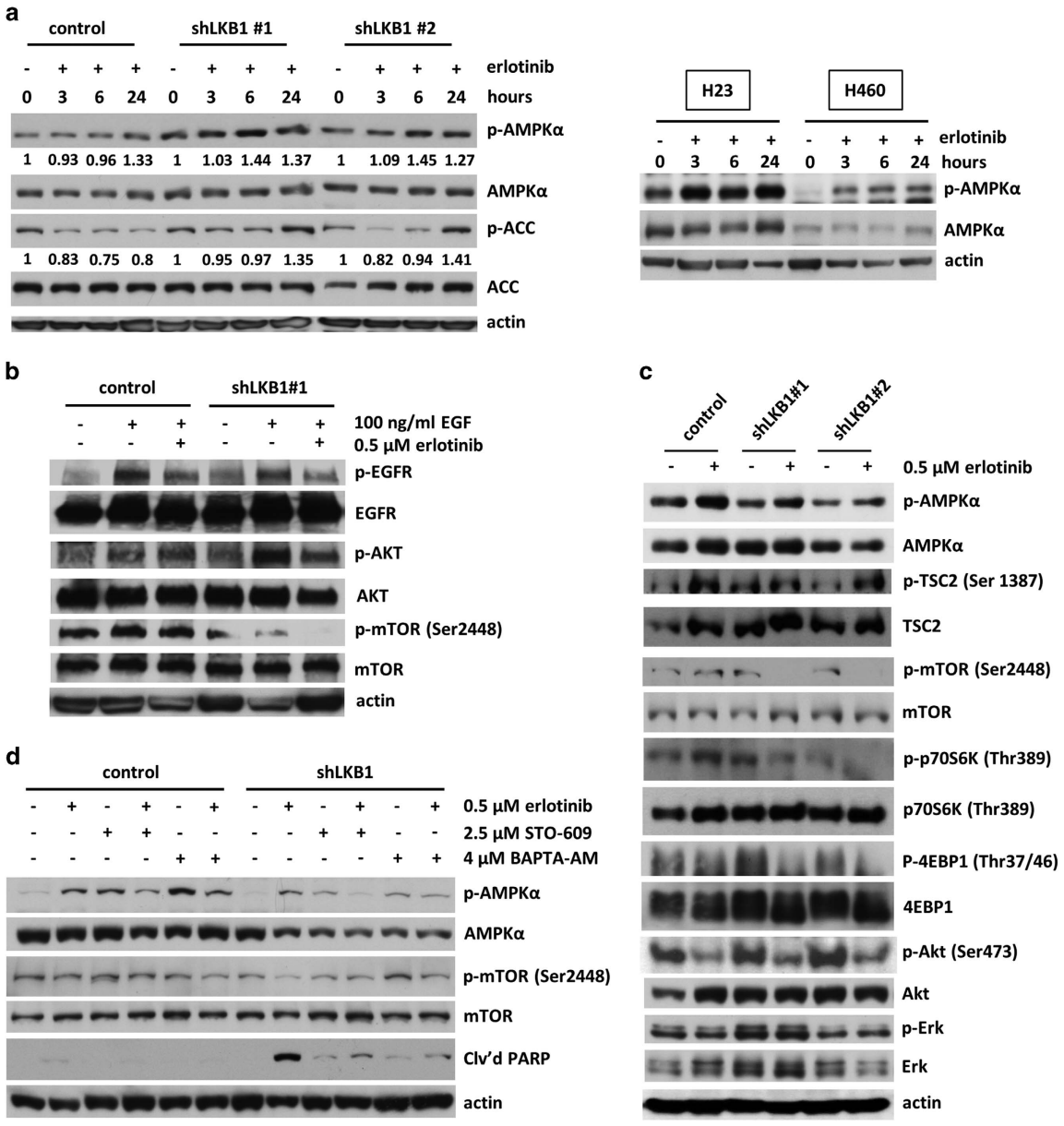

Figure 5. Erlotinib-induced activation of AMPKα selectively inhibits the mTOR signaling pathway in LKB1-deficient cells. (**a**) Left panel: erlotinib activated AMPKα and inhibited ACC in shLKB1 Calu-6 cells. Following treatment with 0.5 μM erlotinib for the indicated time, cell lysates were analyzed by western blotting. The expression of phosphorylated AMPKα was calculated as the ratio of phosphorylated AMPKα to total AMPKα protein expression using densitometric analysis. The ratio of phosphorylated to total ACC was calculated similarly. All expression ratios were normalized to the untreated group. Right panel: erlotinib also induced phosphorylated AMPKα in LKB1 mutant H23 and H460 cells. (**b**) Erlotinib inhibited EGF-stimulated EGFR phosphorylation and mTOR phosphorylation in shLKB1 Calu-6 cells. Cells were treated with 0.5 μM erlotinib for 72 h. After serum starvation for 24 h, cells were stimulated by 100 ng/ml EGF for 10 min and cell lysates were then analyzed by western blotting. (**c**) Erlotinib blocked mTOR pathway signaling and activated AMPKα in shLKB1 Calu-6 cells. After 24 h of 0.5 μM erlotinib treatment, cell lysates were analyzed by western blotting using specific antibodies for the indicated proteins. Blockade of mTOR activity following erlotinib treatment resulted in decreased phosphorylation of p70S6K and 4EBP1 in shLKB1 Calu-6 cells. (**d**) Erlotinib-induced AMPKα phosphorylation was reduced by addition of STO-609 (a CAMKKβ inhibitor) or BAPTA-AM (an intracellular calcium chelator) in shLKB1 Calu-6 cells. Cells were co-treated with 0.5 μM erlotinib and 2.5 μM STO-609 or 4 μM BAPTA-AM for 24 h and cell lysates were analyzed by western blotting. The blots are representative of three independent experiments.

Calu-6 cells after 24 h, but shLKB1 cells exhibited complete disruption of mTOR pathway signaling following erlotinib treatment. In particular, AMPKα can directly phosphorylate TSC2 at Ser 1387, which is involved in inhibition of mTOR signaling. shLKB1 Calu-6 cells exhibited enhanced phosphorylation of TSC2 (Ser1387) by erlotinib treatment in comparison with control cells. Furthermore, erlotinib decreased phosphorylation of the 70-kDa ribosomal protein S6 kinase (p70S6K1) and 4EBP-1, both downstream effectors of mTOR signaling. Erlotinib treatment reduced phosphorylation of Akt in all cells, but phosphorylated Erk was not changed. These effects of erlotinib on AMPK and mTOR pathway signaling were further confirmed in H358, A549 and H460 cells. For example, shLKB1 H358 cells exhibited enhanced phosphorylation of AMPKα and inhibition of mTOR signaling in response to erlotinib treatment (Supplementary Figure S4A), whereas LKB1-overexpressing A549 and H460 cells were less

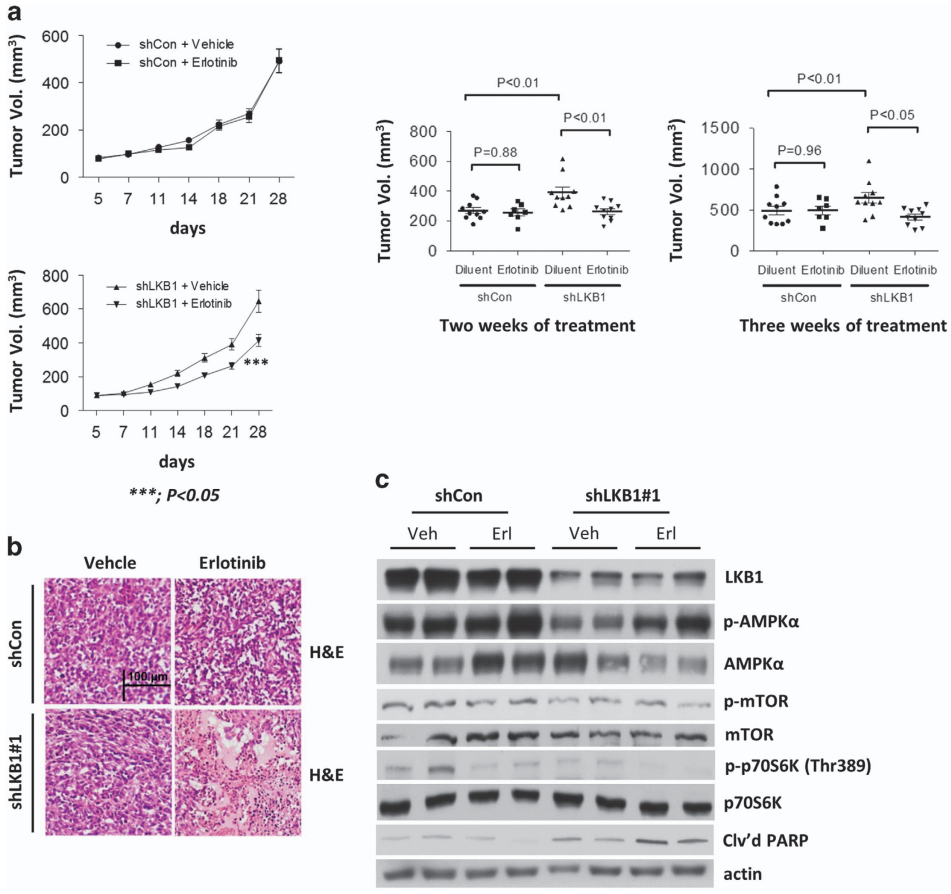

Figure 6. Erlotinib induces a significant reduction of tumor volume in shLKB1 mice. (**a**) Mean tumor volumes for each treatment group of the pLKO.1 control vector (diluent, $n=10$, erlotinib, $n=8$) and shLKB1 vector (diluent, $n=10$, erlotinib, $n=10$) mice after 1 week of treatment. Female nude mice were injected subcutaneously in the left/right flanks with 5×10^6 control or shLKB1 Calu-6 cells per mouse mixed 1:1 with 100% Matrigel. After 7 days, mice were treated with diluent or erlotinib in sodium carboxymethylcellulose and Tween 80 solution orally at 100 mg/kg daily. Body weight was measured twice a week, and drug administration was adjusted accordingly. Tumors were measured twice a week with a caliper. Dots: individual tumor volumes (mm^3). Horizontal lines: median and interquartile ranges. *P*-values are from linear regression analyses and Mann–Whitney *U*-test. (**b**) H&E immunohistochemical staining of sectioned tumor tissues. Original magnification, ×20. Scale bars, 100 μm. **(c)** Erlotinib inhibited mTOR signaling and enhanced cleaved PARP in shLKB1 Calu-6 tumor xenografts. The blots are representative of three independent experiments.

sensitive to mTOR inhibition by erlotinib in comparison with vector control cells (Supplementary Figure S4B). These results indicate that erlotinib induces phosphorylation of AMPKα in both control and LKB1-deficient cells, but its effect to block mTOR pathway signaling is enhanced in LKB1-deficient cells, resulting in repression of protein synthesis and inhibition of cell growth.

We then asked whether an alternative kinase other than LKB1 could be responsible for erlotinib-induced activation of AMPKα in LKB1-deficient cells. In a previous study, it was shown that AMPKα can become phosphorylated in response to energy stress, even in the absence of functional LKB1, through the action of calcium/calmodulin-dependent protein kinase kinase β (CaMKKβ).[33] To elucidate the mechanism by which erlotinib treatment can induce phosphorylation of AMPKα in LKB1-deficient cells, we used STO-609, a CaMKKβ inhibitor, and BAPTA-AM, an intracellular calcium chelator. After 24 h of treatment, both STO-609 and BAPTA-AM were able to partially inhibit erlotinib-induced AMPK phosphorylation in shLKB1 Calu-6 cells (Figure 5d). This partially blocked erlotinib's ability to inhibit mTOR and induce apoptosis in shLKB1 Calu-6 cells. These results indicate that AMPKα activation can be stimulated by erlotinib-induced changes in intracellular ADP/ATP levels and CAMKKβ activity, even in the absence of functional LKB1. This provides a mechanistic explanation for erlotinib's ability to activate AMPKα and suppress mTOR signaling in LKB1-deficient cells.

Erlotinib reduces tumor volume in shLKB1 Calu-6 tumor xenografts

Finally, we investigated the *in vivo* antitumor activity of erlotinib in nude mice bearing control and shLKB1 Calu-6 subcutaneous tumors. As expected, mice bearing shLKB1 Calu-6 tumor xenografts showed the highest tumor volumes (Figure 6a, left panel). Mean tumor volume in mice bearing shLKB1 tumors was significantly reduced at 2–3 weeks of erlotinib treatment, as compared with control-treated mice (Figure 6a, right panel). No toxic effects (such as severe reduction in body weight) were observed in erlotinib-treated groups. We performed histological analyses of tumor samples by H&E immunohistochemical staining and found clear signs of large necrotic areas in shLKB1 tumor xenografts treated with erlotinib, but not in control xenografts (Figure 6b). We also collected tissue samples from tumors to determine the *in vivo* effects of erlotinib treatment on activation of AMPKα, mTOR, p70S6K and cleaved PARP (Figure 6c). We first detected levels of LKB1 expression in control and shLKB1 Calu-6 tumor tissues from mice. As shown by western blotting, levels of LKB1 protein were highly reduced in shLKB1 Calu-6 xenograft

tumors as compared with control tumors. Consistent with *in vitro* results, erlotinib treatment enhanced AMPK phosphorylation, inhibited mTOR-related downstream signaling proteins and increased PARP cleavage in shLKB1 Calu-6 xenograft tumors only. These results suggest that erlotinib treatment significantly reduced tumor growth in shLKB1 Calu-6 tumor xenografts through inhibition of mTOR signaling and induction of apoptosis.

DISCUSSION

Although erlotinib exhibits potent anti-cancer activity against human NSCLC tumors with activating mutations in *EGFR*, it also has activity in some patients with wild-type *EGFR*. It has been unclear as to what molecular mechanisms drive this sensitivity and, further, how to identify wild-type *EGFR* tumors that might be susceptible to erlotinib treatment. In the present study, we found that NSCLC cells harboring wild-type *EGFR* show varying sensitivity to erlotinib treatment that is dependent on *LKB1* status. We demonstrated that erlotinib suppressed viability and enhanced apoptosis of LKB1-deficient NSCLC cells both *in vitro* and *in vivo*. Another study recently reported that glioblastoma cells with wild-type *EGFR* exhibited sensitivity to erlotinib treatment that was associated with inhibition of autophagy but was independent of caspase activity.[34] Consistent with this report, our findings indicate that erlotinib can be beneficial even in tumors that are not *EGFR* mutated. However, we show that apoptosis is elevated in erlotinib-treated cells and that the inhibitory effects of erlotinib are enhanced in tumors that have dysregulated LKB1-AMPK pathway signaling. Because this signaling pathway normally serves to maintain mitochondrial function and bioenergetic homeostasis in response to metabolic stress, we hypothesized that LKB1-deficient cells may be compromised in their ability to cope with metabolic alterations induced by erlotinib treatment.

To further examine the mechanism of erlotinib-induced apoptosis in LKB1-deficient NSCLC cells, we analyzed changes in glycolytic metabolism and mitochondrial function resulting from LKB1 knockdown. Interestingly, we observed that glucose consumption and lactate production by Calu-6 cells increased by more than 50% in response to LKB1 knockdown, which correlated with increased growth and colony formation (Figure 2c). We also observed substantial increases in OCR (Figure 3b) and $\Delta\psi_m$ (Figure 4a) after expression of shLKB1 in Calu-6 and H358 cells, consistent with another recent study that profiled gene expression of over 600 patient tumors and reported upregulation of oxidative phosphorylation and mitochondria-associated genes in samples classified as LKB1-deficient.[23] The effect of LKB1 loss to activate glycolysis and oxidative metabolism was further confirmed by expressing wild-type LKB1 in mutant A549 and H460 cell lines (Figures 2a and b, Supplementary Figures S1 and S2). Faubert *et al.*[32] previously reported simultaneous increases in both glucose uptake and lactate production in response to complete *LKB1* knockout in transgenic mouse embryonic fibroblasts. They also noted enhanced flux of both glucose and glutamine into the TCA cycle of LKB1-mutant A549 cells in comparison with cells expressing wild-type LKB1, on the basis of isotope labeling experiments with ^{13}C-glucose and ^{13}C-glutamine tracers. These previous findings are consistent with our own results indicating increased dependence of LKB1-deficient cells on mitochondrial metabolism to support enhanced cell proliferation.

Despite elevated rates of oxidative metabolism, we observed only slight changes in basal ADP/ATP ratios and ROS levels in LKB1 knockdown cells (Figures 3c and 4b). However, the effect of LKB1 depletion to alter mitochondrial function became readily apparent when shLKB1 cells were challenged with erlotinib. Substantial increases in ADP/ATP and ROS levels were observed, which were accompanied by depletion of $\Delta\psi_m$ (Figure 4a). In contrast, control cells were able to maintain normal ADP/ATP, ROS and $\Delta\psi_m$ levels in response to the same concentration of erlotinib (Figures 3c, 4a and b). Taken together, these data provide a clear indication that LKB1 is required for maintenance of mitochondrial function in the presence of erlotinib treatment. As a result, LKB1-deficient cells cannot effectively restore ATP levels or prevent ROS accumulation in response to erlotinib, resulting in selective growth inhibition (Figure 2) and apoptosis activation (Figures 4c and d). In this context, we view the decoupling of ROS from OCR and $\Delta\psi_m$ measurements as an indicator of mitochondrial dysfunction following erlotinib treatment. These results are similar to those reported by Shackelford *et al.*,[12] where significant increases in ROS and decreases in $\Delta\psi_m$ were simultaneously observed in response to phenformin treatment of LKB1-mutant A549 cells. Our results are also consistent with another previous study that showed that AMPK-deficient cells are unable to maintain sufficient NADPH levels needed to neutralize mitochondrial ROS during metabolic stress,[35] a mechanism that may further contribute to the enhanced erlotinib sensitivity we observed in LKB1-deficient cells.

Despite the previously described similarities, our observations of increased basal mitochondrial activity in LKB1-deficient cells are also partially at odds with the results of Shackelford *et al.*.[12] Their study showed that re-expressing wild-type LKB1 in A549 cells led to enhancements of basal OCR and $\Delta\psi_m$, implying reduced mitochondrial activity in the parental, LKB1-deficient cells.[12] In contrast, a more recent study by Faubert *et al.*[32] showed no change in OCR after re-expressing LKB1 in A549 cells and a reduction in OCR after re-expressing LKB1 in A427 cells, which are also LKB1 mutant type. Therefore, there is some variability in previous studies concerning the effects that manipulating LKB1 expression has on markers of mitochondrial activity. It is possible that these differences could be attributable to adaptation of LKB1 mutant cells to the re-expression of LKB1 over many generations. As our studies were completed within 10 passages following antibiotic selection, our results likely capture the immediate response to LKB1 re-expression in the absence of long-term adaptation.

Another unexpected outcome of our study was that LKB1-deficient cells still exhibited a robust ability to activate AMPK in response to increases in ADP/ATP ratio following erlotinib treatment. AMPK activation by adenine nucleotides involves at least three independent mechanisms: (1) increased AMP-dependent phosphorylation by LKB1; (2) inhibitory effects of AMP on its dephosphorylation; and (3) allosteric activation by AMP and ADP.[36] The latter two mechanisms do not require LKB1. We also found that the ability of erlotinib to induce phosphorylation of AMPKα in LKB1-deficient cells was partially inhibited by co-treatment with either STO-609 or BAPTA-AM (Figure 5d), indicating involvement of CaMKKβ as an alternative kinase that contributes to erlotinib-induced AMPK phosphorylation. Two prior articles have reported that AMPK phosphorylation by CaMKKβ is dependent on AMP and ADP levels.[37,38] The large increase in ADP/ATP ratio that we observed following erlotinib treatment could therefore be sufficient to activate AMPK even when LKB1 was depleted, possibly by a CaMKKβ-dependent mechanism. We cannot rule out, however, that changes in Ca^{2+} levels may synergize with changes in energy charge to stimulate AMPK activation in response to erlotinib treatment. Consistent with this hypothesis, gefitinib has been reported to increase cytosolic and mitochondrial calcium levels of Bcl-2-overexpressing cells.[39]

Erlotinib-mediated AMPKα activation led to inhibition of mTOR phosphorylation in LKB1-deficient cells, which correlated with inhibition of phosphorylated p70S6K and 4EBP-1 (Figure 5c) as major downstream effectors of the mTOR signaling pathway. These data are consistent with the known role of AMPK to suppress mTOR signaling in response to low ATP levels, leading to inhibition of protein synthesis and proliferation of cancer cells.[10,40] Previous studies suggested that loss of LKB1 induced increased cell size and mass due to failure of AMPK to inhibit mTOR

signaling.[32,33] In contrast, we found that only LKB1-deficient cells effectively suppressed mTOR signaling and induced PARP cleavage in response to erlotinib treatments, both *in vitro* and *in vivo*. This led to a significant decrease in growth of LKB1-deficient xenograft tumors. It is likely that mitochondrial dysfunction associated with LKB1 deficiency sensitizes cells to erlotinib treatment by enhancing changes in ADP/ATP and ROS levels, which subsequently activate AMPK and suppress mTOR signaling.

Inhibition of Erk signaling has also been shown to induce pyruvate dehydrogenase kinase 4 (PDK4) expression and redirect cellular metabolism in mammary epithilia.[41] However, we do not expect that changes in Mek/Erk signaling or PDK4 expression were directly involved in regulating the metabolic response to erlotinib treatment in our studies. First, no significant change in Erk phosphorylation was observed in response to erlotinib treatment of Calu-6 cells (Figure 5c, Supplementary Figure S4). Second, if PDK4 expression was induced by erlotinib treatment, we would expect to see increased lactate production due to inhibition of pyruvate dehydrogenase flux. However, this was not observed in any of the cell lines tested. Finally, to confirm these observations, we performed western blot analysis with an anti-PDK4 antibody in LKB1-overexpressing and stable knockdown cell lines (Supplementary Figure S5). No significant changes in PDK4 expression were observed after 24 h of erlotinib treatment. Taken together, we conclude that erlotinib treatment reduces OCR in LKB1-deficient cells independently of Erk and PDK4.

In conclusion, we demonstrate for the first time that erlotinib induces apoptosis in *EGFR* wild-type NSCLC cells by a mechanism that is enhanced by LKB1 loss of function (Figure 7). Although LKB1-deficient cells relied more heavily on mitochondrial oxidative phosphorylation for energy production under basal conditions, they could not properly respond to metabolic stress induced by erlotinib treatment in order to maintain energetic homeostasis. These metabolic alterations were associated with more pronounced AMPK activation and inhibition of mTOR signaling in LKB1-deficient cells, resulting in increased sensitivity to erlotinib treatment. Taken together, our findings provide a rationale for erlotinib treatment of LKB1-deficient NSCLC tumors, even in the absence of EGFR activating mutations. These tumors may constitute a distinct NSCLC molecular subtype with enhanced erlotinib sensitivity, which motivates the development of novel diagnostic approaches (for example, mRNA expression profiling[23]) capable of identifying LKB1-deficient patient tumors that are potentially susceptible to erlotinib treatment.

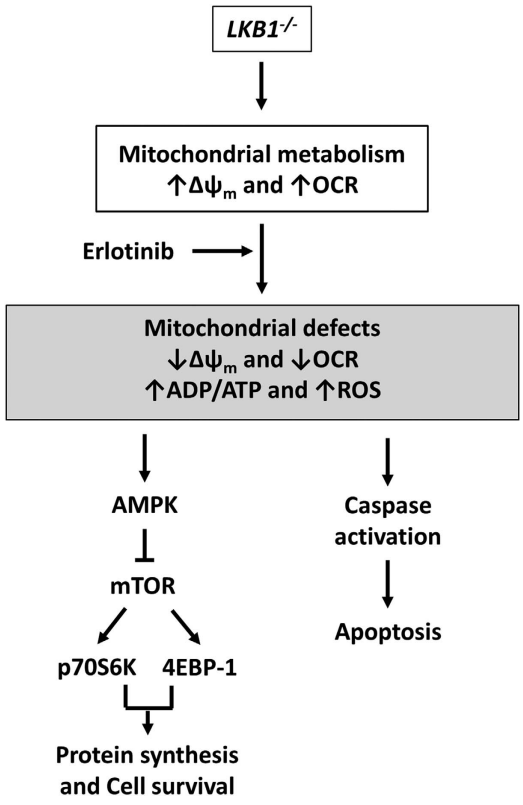

Figure 7. Hypothetical schema of erlotinib-induced cell death in LKB1-deficient cells. LKB1-deficient cells exhibit enhanced mitochondrial metabolism, as indicated by increased mitochondrial potential and OCR. Erlotinib treatment selectively induces mitochondrial dysfunction in LKB1-deficient cells, decreasing mitochondrial potential and OCR while increasing ADP/ATP and ROS. This has the dual effect of inhibiting growth (via activation of AMPK and suppression of mTOR signaling) and activating apoptosis. This mechanism is based on composite data from our *in vitro* studies on multiple LKB1 wild-type (Calu-6, H358) and LKB1 mutant (A549, H460) cell lines, as well as *in vivo* data from Calu-6 mouse xenografts.

MATERIALS AND METHODS

Cell culture and reagents

Human NSCLC Calu-6, H358, H2009, H460, H23, H2122, HCC15 and A549 cell lines were generously shared with us by John Minna and Luc Girard (University of Texas Southwestern Medical Center, Dallas, TX, USA). Cells were tested to ensure that they were mycoplasma negative. The human NSCLC cells were maintained in RPMI 1640 medium supplemented with 10% fetal bovine serum (FBS; GIBCO-BRL, Gaithersburg, MD, USA) in a humidified atmosphere with 5% CO_2. A549 and H460 cells stably expressing either an empty pBABE vector (vector) or wild-type LKB1 (LKB1) were generated by retroviral transduction. The empty pBABE viral plasmid and pBABE-LKB1 plasmid were obtained from Addgene (Cambridge, MA, USA). Phoenix cells were transfected with viral plasmids, and retroviral particles were harvested from media supernatant 48 h after transfection. Viruses were added to target cells with polybrene, and selection with 1 μg/ml puromycin was begun 48–72 h after infection. Cells were selected under puromycin for 1–2 weeks before performing subsequent experiments, with experiments being completed within 2 months. Erlotinib (an inhibitor of EGFR), LY294002 (an inhibitor of PI3K) and rapamycin (an inhibitor of mTOR) were purchased from LC Laboratories (Woburn, MA, USA).

Cell viability analysis, colony formation assays and growth rate measurements

Cells were plated in 96-well plates in complete medium and treated with various concentrations of erlotinib, LY294002 or rapamycin. Cell viability was analyzed after 2 days of treatment using the 3-(4,5-dimethylthiazol-2-yl)-2,5-diphenyltetrazolium bromide (MTT) assay according to the manufacturer's instructions (Sigma, St Louis, MO, USA). Cell proliferation was analyzed every 8 or 16 h for 3 days after erlotinib treatment using the CyQUANT Direct Cell Proliferation Assay according to the manufacturer's protocol (Invitrogen, Frederick, MD, USA). The fluorescence intensity was measured with a fluorescence microplate reader (Bio-Tek Instruments, Winooski, VT, USA). Conditioned medium samples were collected from each well before CyQUANT analysis, frozen, and stored for metabolite analysis. Colony formation assays were performed following treatment with 5 μM erlotinib for 3 days, at which time the cells were replated in six-well plates at low density (1×10^3 cells per well) in complete medium for 2 weeks. Colonies were fixed with methanol and stained with 0.1% crystal violet (Sigma-Aldrich). Colony numbers were assessed visually and colonies measuring at least 50 μm were counted.

Metabolite analysis and oxygen consumption rate

Conditioned medium samples collected during cell growth experiments were subjected to glucose and lactate analysis using a YSI 2300 biochemical analyzer (YSI Life Science, Yellow Springs, OH, USA). The ETA software package was applied to calculate specific rates of glucose consumption and lactate production using an exponential growth

model.[42] OCR was measured using the Oxygraph-2K (Oroboros, Innsbruck, Austria), which contains two chambers with separate oxygen probes to monitor online changes in oxygen concentration. The instrument was set to a temperature of 37 °C, and the stirring speed for each chamber was 750 r.p.m. After treatment with erlotinib for 24 h, cells were trypsinized, resuspended in the same culture medium at a concentration of $1–2 \times 10^6$ cells per ml and injected into the Oxygraph instrument.

LKB1 stable knockdown using lentiviral short-hairpin RNA

For generation of stable knockdown cells, lentiviral LKB1 short-hairpin RNA (shRNA) constructs and a non-targeting shRNA control were purchased from Open Biosystems (Huntsville, AL, USA). These constructs were cloned into a pLKO.1 vector. HEK293T cells (2×10^6 cells) were plated on 100 mm dishes and 1 day later were co-transfected with 5 μg shRNA constructs, 3 μg pCMV-dR8.2 dvpr (Addgene) and 2 μg pCMV-VSV-G (Addgene) using a calcium phosphate transfection kit (Invitrogen). After 6 h, the medium was exchanged with fresh medium, and then the viral stock was collected for 1–2 days and filtered to remove non-adherent HEK293T cells. To obtain stable shRNA-expressing clones, Calu-6 or H358 cells were plated on six-well plates, and 1 day later infected with 1 ml of lentiviral suspension plus 4 μg/ml polybrene. Puromycin selection (0.5–2 μg/ml) was initiated 2 days after lentiviral infection.

Western blotting

Total cell lysates were resolved using sodium dodecyl sulfate-polyacrylamide gel electrophoresis and then transferred onto polyvinylidene fluoride membranes (EMD Millipore Corporation, Billerica, MA, USA). Western blotting was performed as described previously.[43] The following antibodies were purchased from Cell Signaling (Danvers, MA, USA): rabbit polyclonal antibodies against LKB1, phosphorylated AMPKα, phosphorylated ACC, phosphorylated Tuberin/TSC2 (Ser1387), phosphorylated mTOR (Ser2448), phosphorylated 4EBP1 (Thr37/46), phosphorylated Akt (Ser473), phosphorylated Erk (Thr202/Tyr204), PARP, and mouse monoclonal antibodies against phosphorylated p70S6K (Thr389). A goat polyclonal anti-actin antibody was purchased from Santa Cruz (Santa Cruz, CA,USA). All experiments were performed in triplicate.

Flow cytometry

Cells were seeded in six-well plates containing complete medium and treated with 5 μM or 10 μM erlotinib. After 72 h, cells were harvested, pooled, and fixed with 1% paraformaldehyde and 70% ethanol. Apoptosis was assessed with flow cytometry using the Annexin V-FITC Apoptosis kit (Clontech, Mountain View, CA, USA). To measure mitochondrial ROS after 24 h of erlotinib treatment, cells were stained with MitoSOX Red (Molecular Probes, Eugene, OR, USA) for 40 min at 37 °C in the dark. Annexin V and MitoSOX Red were analyzed using a LSRII flow cytometer (Becton Dickinson, San Jose, CA, USA).

Assessment of ADP/ATP ratio and mitochondrial membrane potential

Cells were seeded in 96-well plates and treated with 25 μM erlotinib for 24 h. Intracellular ADP/ATP ratio was measured using a bioluminescent ADP/ATP Ratio Assay Kit according to the manufacturer's instructions (Abcam, Cambridge, MA, USA). Mitochondrial membrane depolarization was determined using the JC-1 fluorescence probe according to the manufacturer's instructions (Molecular Probes). Cells were labeled with 2 μM JC-1 for 30 min at 37 °C in the dark and then analyzed at 488 nm excitation with 530/30 or 585/42 nm bypass emission filters using a fluorescence microplate reader (Bio-TeK Instruments).

Animal experiments

The research protocol for animal studies was approved by and carried out in accordance with the Vanderbilt Institutional Animal Care & Use Committee. Female *Foxn1*$^{nu/nu}$ nude mice aged 4–5 weeks were purchased from Harlan Laboratories (Indianapolis, IN, USA). Both non-targeting shRNA (shCon, LKB1 wild-type) and LKB1 shRNA (shLKB1, LKB1 knockdown) Calu-6 cells were injected subcutaneously into the left/right flanks at 5×10^6 cells per mouse mixed 1:1 with 100% growth factor-reduced Matrigel (BD Bioscience, San Jose, CA, USA). The mice were randomly assigned to shCon +vehicle solution (in sodium carboxymethylcellulose and Tween 80), shCon +erlotinib, shLKB1+ vehicle solution and shLKB1+erlotinib, with each group containing 8–10 mice. After 1 week, mice were treated with vehicle or erlotinib (100 mg/kg) daily by oral gavage for 3 weeks. Tumor size was calculated by measuring the tumors in three dimensions using calipers twice a week,[44] and body weight was measured twice weekly. On day 21, mice were euthanized and tumor tissues were harvested for pathologic examination (immunohistochemical analysis) and analyzed by western blotting.

Statistical analyses

The data acquired with MTT, colony formation and ADP/ATP assays were analyzed using the Student *t*-test. The Mann–Whitney *U*-test was used to compare differences in tumor weight. In all of the statistical analyses, two-sided *P*-values < 0.05 were considered statistically significant.

CONFLICT OF INTEREST

The authors declare no conflict of interest.

ACKNOWLEDGEMENTS

This work was supported by NIH P50 CA090949, DOD W81XWH-12-1-0383, NSF CBET-1105991, and by an award from Uniting Against Lung Cancer. Dr Joshua P. Fessel was also supported by NIH K08 HL121174. The authors thank Dr Changki Lee for his assistance with the animal experiments.

REFERENCES

1 Jemal A, Siegel R, Xu J, Ward E. Cancer statistics, 2010. *CA Cancer J Clin* 2010; **60**: 277–300.
2 Rapp E, Pater JL, Willan A, Cormier Y, Murray N, Evans WK *et al.* Chemotherapy can prolong survival in patients with advanced non-small-cell lung cancer--report of a Canadian multicenter randomized trial. *J Clin Oncol* 1988; **6**: 633–641.
3 West L, Vidwans SJ, Campbell NP, Shrager J, Simon GR, Bueno R *et al.* A novel classification of lung cancer into molecular subtypes. *PLoS One* 2012; **7**: e31906.
4 Kwak EL, Bang YJ, Camidge DR, Shaw AT, Solomon B, Maki RG *et al.* Anaplastic lymphoma kinase inhibition in non-small-cell lung cancer. *N Engl J Med* 2010; **363**: 1693–1703.
5 Tsao MS, Sakurada A, Cutz JC, Zhu CQ, Kamel-Reid S, Squire J *et al.* Erlotinib in lung cancer - molecular and clinical predictors of outcome. *N Engl J Med* 2005; **353**: 133–144.
6 Shackelford DB, Shaw RJ. The LKB1-AMPK pathway: metabolism and growth control in tumour suppression. *Nat Rev Cancer* 2009; **9**: 563–575.
7 Sanchez-Cespedes M, Parrella P, Esteller M, Nomoto S, Trink B, Engles JM *et al.* Inactivation of LKB1/STK11 Is a common event in adenocarcinomas of the lung. *Cancer Res* 2002; **62**: 3659–3662.
8 Ji H, Ramsey MR, Hayes DN, Fan C, McNamara K, Kozlowski P *et al.* LKB1 modulates lung cancer differentiation and metastasis. *Nature* 2007; **448**: 807–810.
9 Hardie DG, Ross FA, Hawley SA. AMPK: a nutrient and energy sensor that maintains energy homeostasis. *Nat Rev Mol Cell Biol* 2012; **13**: 251–262.
10 Mihaylova MM, Shaw RJ. The AMPK signalling pathway coordinates cell growth, autophagy and metabolism. *Nat Cell Biol* 2011; **13**: 1016–1023.
11 Carretero J, Medina PP, Blanco R, Smit L, Tang M, Roncador G *et al.* Dysfunctional AMPK activity, signalling through mTOR and survival in response to energetic stress in LKB1-deficient lung cancer. *Oncogene* 2007; **26**: 1616–1625.
12 Shackelford DB, Abt E, Gerken L, Vasquez DS, Seki A, Leblanc M *et al.* LKB1 inactivation dictates therapeutic response of non-small cell lung cancer to the metabolism drug phenformin. *Cancer Cell* 2013; **23**: 143–158.
13 Faber AC, Li D, Song Y, Liang M-C, Yeap BY, Bronson RT *et al.* Differential induction of apoptosis in HER2 and EGFR addicted cancers following PI3K inhibition. *Proc Natl Acad Sci USA* 2009; **106**: 19503–19508.
14 Pao W, Miller V, Zakowski M, Doherty J, Politi K, Sarkaria I *et al.* EGF receptor gene mutations are common in lung cancers from "never smokers" and are associated with sensitivity of tumors to gefitinib and erlotinib. *Proc Natl Acad Sci USA* 2004; **101**: 13306–13311.
15 Sharma SV, Bell DW, Settleman J, Haber DA. Epidermal growth factor receptor mutations in lung cancer. *Nat Rev Cancer* 2007; **7**: 169–181.
16 Shepherd FA, Rodrigues Pereira J, Ciuleanu T, Tan EH, Hirsh V, Thongprasert S *et al.* Erlotinib in previously treated non–small-cell lung cancer. *N Engl J Med* 2005; **353**: 123–132.
17 Cappuzzo F, Ciuleanu T, Stelmakh L, Cicenas S, Szczésna A, Juhász E *et al.* Erlotinib as maintenance treatment in advanced non-small-cell lung cancer: a multicentre, randomised, placebo-controlled phase 3 study. *Lancet Oncol* 2010; **11**: 521–529.

18 Garassino MC, Marsoni S, Floriani I. Testing epidermal growth factor receptor mutations in patients with non–small-cell lung cancer to choose chemotherapy: the other side of the coin. *J Clin Oncol* 2011; **29**: 3835–3837.
19 Deng J, Shimamura T, Perera S, Carlson NE, Cai D, Shapiro GI *et al.* Proapoptotic BH3-Only BCL-2 family protein BIM connects death signaling from epidermal growth factor receptor inhibition to the mitochondrion. *Cancer Res* 2007; **67**: 11867–11875.
20 Ling Y-H, Lin R, Perez-Soler R. Erlotinib induces mitochondrial-mediated apoptosis in human H3255 non-small-cell lung cancer cells with epidermal growth factor receptorl858r mutation through mitochondrial oxidative phosphorylation-dependent activation of BAX and BAK. *Mol Pharmacol* 2008; **74**: 793–806.
21 Nakada D, Saunders TL, Morrison SJ. Lkb1 regulates cell cycle and energy metabolism in haematopoietic stem cells. *Nature* 2010; **468**: 653–658.
22 Matsumoto S, Iwakawa R, Takahashi K, Kohno T, Nakanishi Y, Matsuno Y *et al.* Prevalence and specificity of LKB1 genetic alterations in lung cancers. *Oncogene* 2007; **26**: 5911–5918.
23 Kaufman JM, Amann JM, Park K, Arasada RR, Li H, Shyr Y *et al.* LKB1 loss induces characteristic patterns of gene expression in human tumors associated with NRF2 activation and attenuation of PI3K-AKT. *J Thorac Oncol* 2014; **9**: 794–804.
24 Van Schaeybroeck S, Kyula J, Kelly DM, Karaiskou-McCaul A, Stokesberry SA, Van Cutsem E *et al.* Chemotherapy-induced epidermal growth factor receptor activation determines response to combined gefitinib/chemotherapy treatment in non–small cell lung cancer cells. *Mol Cancer Ther* 2006; **5**: 1154–1165.
25 Tracy S, Mukohara T, Hansen M, Meyerson M, Johnson BE, Jänne PA. Gefitinib induces apoptosis in the EGFRL858R non–small-cell lung cancer cell line H3255. *Cancer Res* 2004; **64**: 7241–7244.
26 Onozato R, Kosaka T, Achiwa H, Kuwano H, Takahashi T, Yatabe Y *et al. LKB1* gene mutations in Japanese lung cancer patients. *Cancer Sci* 2007; **98**: 1747–1751.
27 Liu Y, Marks K, Cowley GS, Carretero J, Liu Q, Nieland TJF *et al.* Metabolic and functional genomic studies identify deoxythymidylate kinase as a target in LKB1-mutant lung cancer. *Cancer Discov* 2013; **3**: 870–879.
28 Mahoney CL, Choudhury B, Davies H, Edkins S, Greenman C, Haaften G *et al.* LKB1/KRAS mutant lung cancers constitute a genetic subset of NSCLC with increased sensitivity to MAPK and mTOR signalling inhibition. *Br J Cancer* 2009; **100**: 370–375.
29 Woods A, Johnstone SR, Dickerson K, Leiper FC, Fryer LGD, Neumann D *et al.* LKB1 is the upstream kinase in the AMP-activated protein kinase cascade. *Curr Biol* 2003; **13**: 2004–2008.
30 Shaw RJ, Kosmatka M, Bardeesy N, Hurley RL, Witters LA, DePinho RA *et al.* The tumor suppressor LKB1 kinase directly activates AMP-activated kinase and regulates apoptosis in response to energy stress. *Proc Natl Acad Sci USA* 2004; **101**: 3329–3335.
31 Sanders MJ, Grondin PO, Hegarty BD, Snowden MA, Carling D. Investigating the mechanism for AMP activation of the AMP-activated protein kinase cascade. *Biochem J* 2007; **403**: 139–148.
32 Faubert B, Vincent EE, Griss T, Samborska B, Izreig S, Svensson RU *et al.* Loss of the tumor suppressor LKB1 promotes metabolic reprogramming of cancer cells via HIF-1alpha. *Proc Natl Acad Sci USA* 2014; **111**: 2554–2559.
33 Hurley RL, Anderson KA, Franzone JM, Kemp BE, Means AR, Witters LA. The Ca2 +/Calmodulin-dependent protein kinase kinases are AMP-activated protein kinase kinases. *J Biol Chem* 2005; **280**: 29060–29066.
34 Eimer S, Belaud-Rotureau M-A, Airiau K, Jeanneteau M, Laharanne E, Véron N *et al.* Autophagy inhibition cooperates with erlotinib to induce glioblastoma cell death. *Cancer Biol Ther* 2011; **11**: 1017–1027.
35 Jeon SM, Chandel NS, Hay N. AMPK regulates NADPH homeostasis to promote tumour cell survival during energy stress. *Nature* 2012; **485**: 661–665.
36 Gowans GJ, Hawley SA, Ross FA, Hardie DG. AMP is a true physiological regulator of AMP-activated protein kinase by both allosteric activation and enhancing net phosphorylation. *Cell Metab* 2013; **18**: 556–566.
37 Oakhill JS, Steel R, Chen ZP, Scott JW, Ling N, Tam S *et al.* AMPK is a direct adenylate charge-regulated protein kinase. *Science* 2011; **332**: 1433–1435.
38 Oakhill JS, Chen ZP, Scott JW, Steel R, Castelli LA, Ling N *et al.* beta-Subunit myristoylation is the gatekeeper for initiating metabolic stress sensing by AMP-activated protein kinase (AMPK). *Proc Natl Acad Sci USA* 2010; **107**: 19237–19241.
39 Zannetti A, Iommelli F, Fonti R, Papaccioli A, Sommella J, Lettieri A *et al.* Gefitinib induction of *in vivo* detectable signals by Bcl-2/Bcl-xL modulation of inositol trisphosphate receptor type 3. *Clin Cancer Res* 2008; **14**: 5209–5219.
40 Shaw RJ, Bardeesy N, Manning BD, Lopez L, Kosmatka M, DePinho RA *et al.* The LKB1 tumor suppressor negatively regulates mTOR signaling. *Cancer Cell* 2004; **6**: 91–99.
41 Grassian AR, Metallo CM, Coloff JL, Stephanopoulos G, Brugge JS. Erk regulation of pyruvate dehydrogenase flux through PDK4 modulates cell proliferation. *Genes Dev* 2011; **25**: 1716–1733.
42 Murphy TA, Young JD. ETA: Robust software for determination of cell specific rates from extracellular time courses. *Biotechnol Bioeng* 2013; **110**: 1748–1758.
43 Whang YM, Kim YH, Kim JS, Yoo YD. RASSF1A suppresses the c-Jun-NH2-kinase pathway and inhibits cell cycle progression. *Cancer Res* 2005; **65**: 3682–3690.
44 Park SI, Lee C, Sadler WD, Koh AJ, Jones J, Seo JW *et al.* Parathyroid hormone–related protein drives a CD11b+Gr1+ cell–mediated positive feedback loop to support prostate cancer growth. *Cancer Res* 2013; **73**: 6574–6583.

Supplementary Information accompanies this paper on the Oncogene website (http://www.nature.com/onc)